Anisotropic skyrmion liquid phase

Daniel Schick [1,*] Tim Matthies [2] Thomas Mutschler [1] Levente Rózsa [3,4] and Ulrich Nowak [1]

[1]*Fachbereich Physik, Universität Konstanz, DE-78457 Konstanz, Germany*

[2]*Department of Physics, University of Hamburg, DE-20355 Hamburg, Germany*

[3]*Department of Theoretical Solid State Physics, Institute of Solid State Physics and Optics, HUN-REN Wigner Research Centre for Physics, H-1525 Budapest, Hungary*

[4]*Department of Theoretical Physics, Budapest University of Technology and Economics, Műegyetem rakpart 3, H-1111 Budapest, Hungary*

(Received 9 December 2025; accepted 2 April 2026; published 11 May 2026)

The nature of the melting transition in two-dimensional systems of particles has attracted considerable research attention since the development of Kosterlitz-Thouless-Halperin-Nelson-Young theory. The hexatic phase proposed by this theory has been recently identified experimentally in ensembles of magnetic skyrmions, quasiparticles formed in a magnetically ordered crystal. Here, we use quasiparticle dynamical simulations to study how the anisotropy of the skyrmion-skyrmion interactions induced by the atomic lattice influences the melting transition. For isotropic interactions, we find a transition from a solid phase through a hexatic phase stable in a narrow temperature range to an isotropic liquid phase. However, if the interactions between skyrmions are forced to be anisotropic by the atomic lattice, then a direct solid-liquid transition can be observed with orientational order persisting up to temperatures of 30 K in the liquid phase.

DOI: 10.1103/qh5x-8lz3

I. INTRODUCTION

Phase transitions in ensembles of particles have been studied extensively in a wide variety of physical systems. In three-dimensional materials, crystals displaying long-ranged positional and orientational order of the particles melt into isotropic liquids where only short-ranged correlations are present through a first-order transition. In two dimensions, the presence of a third phase of matter was proposed, the hexatic phase with short-range positional and long-range orientational order between the quasi-long-range-ordered solid and the isotropic liquid phases. The phase transitions between these three phases are continuous according to the Kosterlitz-Thouless-Halperin-Nelson-Young (KTHNY) theory [1–4]. This theory also establishes that the unbinding of topological defects, including dislocations and disclinations, provides the microscopic mechanism for these phase transitions. It was later recognized that even if the hexatic phase is present, it may be separated from the liquid or the solid state by a first-order transition instead of the second-order one predicted by the KTHNY theory [5,6]. Which of these scenarios is realized in a system depends on the microscopic details, for example, the presence or absence of an underlying periodic potential [2,3], whether the interactions between the particles are repulsive at all distances or contain a region of attraction [5], and how fast this interaction decays with the distance [7]. While most studies have focused on particles with circularly symmetric interaction potentials, various phase transitions have been identified in ensembles of noncircular hard particles in simulations [8,9] and experiments [10]. The nature of these phase transitions has stimulated a considerable amount of theoretical and simulation studies, as well as experimental works where the hexatic phase has been identified in systems of electrons [11], atoms [12], molecules forming liquid crystals [13], colloidal particles [14–17], superconducting vortices [18,19], and vortices in a quasi-two-dimensional Bose gas [20].

Magnetic skyrmions are localized spin configurations in magnetically ordered crystals [21–24]. They are exceptionally stable against perturbations, making it possible to treat them as quasiparticles with a conserved particle number. Skyrmions form a triangular lattice in the ground state, corresponding to a solid phase at finite temperature, which melts into a liquid state as the temperature is increased. Experimental studies have also identified an intermediate hexatic phase between these phases [25–27]. However, skyrmions differ from other particles for which two-dimensional melting has been studied in several aspects. First, the skyrmions are formed on an underlying lattice of magnetic atoms. Therefore, they interact with defects in the atomic lattice [28], and they also experience a periodic potential due to this lattice. If the size of skyrmions is comparable to the atomic separation, this periodic potential can become sufficiently strong to exclude the formation of a hexatic phase, as was found in numerical simulations of the melting transition [29]. Second, skyrmions are characterized by a topological charge influencing their

*Contact author: daniel.schick@uni-konstanz.de

dynamics, which also affects the velocity of defects in the skyrmion crystal that determines how fast the melting occurs [30]. Third, the size of skyrmions, thereby the strength of the interaction between them, may be adjusted by the external magnetic field, which can be utilized to drive the phase transitions [26,27]. Fourth, the underlying microscopic interactions between the spins determine the effective interaction potential between the skyrmions. Studies of the melting transition so far have focused on skyrmions repulsing each other at all distances [26,27,29], which are stabilized by the Dzyaloshinsky-Moriya interaction [31–33]. However, skyrmions stabilized by the competition between ferromagnetic and antiferromagnetic isotropic exchange interactions also exhibit attraction at certain distances [34], and the interaction between them may be strongly anisotropic due to the underlying atomic lattice [35].

Here, we study the influence of the anisotropic interaction between the skyrmions on the melting of the skyrmion lattice. We determine the interaction potential from atomistic spin interactions describing the $(Pt_{0.95}Ir_{0.05})$/Fe/Pd(111) system. We use this anisotropic interaction potential and its isotropic counterpart to perform Brownian dynamics simulations of skyrmions at temperatures up to 30 K in increments of at most 1 K. We calculate positional and orientational order parameters, as well as the numbers of dislocations and disclinations, to characterize the transitions. We find that the anisotropy induced by the underlying atomic lattice acts as an agent promoting positional and orientational order, similarly to how magnetic or electric fields may be used to align magnetic or electric dipoles, or alignment layers at the surfaces of liquid crystals stabilize the orientation of the molecules. Consequently, the anisotropic interactions stabilize the solid phase up to higher temperature than the isotropic interactions, while orientational order remains observable up to the highest simulated temperatures in the liquid phase despite the presence of a large number of topological lattice defects. We compare the phases determined from the correlation functions to a machine-learning classification of the observed spin configurations.

II. METHODS

A. Atomistic spin model

We consider the $(Pt_{0.95}Ir_{0.05})$/Fe/Pd(111) system in our simulations. The magnetic Fe atoms are described by the atomistic spin Hamiltonian

$$\mathcal{H} = \frac{1}{2}\sum_{i\neq j} \boldsymbol{S}_i \mathcal{J}_{ij} \boldsymbol{S}_j + \sum_i \boldsymbol{S}_i \mathcal{K} \boldsymbol{S}_i - \mu_S \sum_i \boldsymbol{S}_i \cdot \boldsymbol{B}, \quad (1)$$

with the exchange interaction tensors $\mathcal{J}_{ij}$, the anisotropy tensor $\mathcal{K}$, external magnetic field $\boldsymbol{B}$, and magnetic spin moment μ_S. The material parameters were determined from first-principles calculations in Ref. [35], and are also reported in Ref. [36]. The lattice constant of the triangular lattice formed by the Fe atoms is $a = 2.751$ Å. We apply an out-of-plane magnetic field of $B = 1$ T, where skyrmions exist as metastable quasiparticles in a field-polarized ground state. We determine the interaction potential by inserting two skyrmions in the collinear background, fixing the centers of the skyrmions at certain lattice sites by aligning the spins at those sites opposite to the external field, and relax all other spin directions at zero temperature using atomistic spin-dynamics simulations until a local energy minimum is reached. We set the zero of the potential energy at the point where the skyrmions are sufficiently far away that the interaction becomes negligible.

B. Dynamical simulations

Neglecting the internal degrees of freedom of skyrmions in a rigid-body approximation, their dynamics as quasiparticles is governed by the Thiele equation [37],

$$\boldsymbol{\mathcal{G}} \times \boldsymbol{v}_i + \alpha \mathcal{D} \boldsymbol{v}_i = \boldsymbol{F}_i, \quad (2)$$

where $\boldsymbol{\mathcal{G}} = \mathcal{G}\boldsymbol{e}_\perp$ is the gyrocoupling vector, $\mathcal{D}$ is the dissipation coefficient, and α is the Gilbert damping known from the Landau-Lifshitz-Gilbert equation. We use the parameters $\mathcal{G}/k_\mathrm{B} = 2.272$ ns K nm^{-2} and $\mathcal{D}/k_\mathrm{B} = 3.396$ ns K nm^{-2} determined in Ref. [38], and $\alpha = 0.1$. On the right-hand side of the equation, the force $\boldsymbol{F}_i$ acting on the skyrmion comprises a term from the skyrmion-skyrmion interaction $\boldsymbol{F}_{i,\mathrm{sk\text{-}sk}}$ and thermal fluctuations $\boldsymbol{F}_{i,\mathrm{th}}$. The thermal force is modeled as Gaussian white noise with expectation value $\langle \boldsymbol{F}_i(t)\rangle = 0$ and covariance $\langle F_i^\mu(t) F_j^\nu(t')\rangle = 2\alpha k_\mathrm{B} T \mathcal{D}_{\mu\nu}\delta_{ij}\delta(t-t')$. The quasiparticle description is assumed to hold within the considered temperature range. For sufficiently high temperatures (above 50 K for the considered material [39]), thermal fluctuations are expected to destabilize the skyrmion configuration, invalidating the quasiparticle approximation on the timescale of the simulations performed here.

The equation of motion is solved numerically for 16 680 interacting skyrmions in a box size of 272.9 nm × 273.4 nm with periodic boundary conditions. The system is thermalized for 25.37 ns before the equilibrium properties are extracted by averaging over 120.8 ns.

C. Description of phase transitions

The KTHNY theory describes the melting process through the unbinding of topological lattice defects. These are identified in our simulations by counting the number of neighbors of each skyrmion in a given configuration via Voronoi tessellation. In a close-packed configuration, all skyrmions have six neighbors. Moving two next-nearest-neighboring skyrmions closer to each other results in two skyrmions with seven neighbors and two skyrmions with five neighbors forming a topologically trivial defect known as a dislocation pair. These defects may split into pairs of skyrmions with five and seven neighbors known as dislocations. Dislocations are characterized by the Burgers vector and are topologically nontrivial; they may only vanish if two dislocations with opposite Burgers vector merge. A single skyrmion with a number of neighbors different from six, where each of its neighbors has six neighbors, is known as a disclination.

Identifying the neighbors of each skyrmion makes it possible to calculate the orientational bond-order parameter

$$\Psi_6(\boldsymbol{r}_i) = \frac{1}{n_i}\sum_j e^{-6\mathrm{i}\theta_{ij}}, \quad (3)$$

which is calculated for skyrmion i by an average over all of its neighbors j, where the angle θ_{ij} is defined between the relative position $\boldsymbol{r}_j - \boldsymbol{r}_i$ and a fixed reference direction in the plane [6]. The spatial and temporal orientational correlation functions are defined as [40,41]

$$g_6(|\boldsymbol{r}_i - \boldsymbol{r}_j|) = \langle \Psi_6^*(\boldsymbol{r}_i)\Psi_6(\boldsymbol{r}_j)\rangle, \tag{4}$$

$$g_6(t_2 - t_1) = \langle \Psi_6^*(t_2)\Psi_6(t_1)\rangle, \tag{5}$$

while the positional order can be characterized by the pair correlation function [41]

$$g(r) = \frac{A}{4\pi r N^2}\left\langle \sum_i \sum_{j\neq i} \delta(r - r_{ij})\right\rangle, \tag{6}$$

where A is the system area, $N$is the number of skyrmions, and r_{ij} is the distance between skyrmions i and j. We further characterize the positional correlations by calculating the structure factor

$$S(\boldsymbol{k}) = \frac{1}{N}\left\langle \left| \sum_{i,j} e^{-i\boldsymbol{k}\cdot(\boldsymbol{r}_i - \boldsymbol{r}_j)} \right| \right\rangle \tag{7}$$

in reciprocal space.

In the solid phase, one finds quasi-long-ranged positional order, with the pair correlation showing algebraic decay ($g(r) \propto r^{-\nu}$), whereas the orientational correlation reaches a finite value at $r \to \infty$. This implies the existence of a global order and thus a finite value for the average bond order $|\langle\Psi_6\rangle|$, which vanishes in phases with finite orientational correlation length. In the hexatic phase, positional order is short ranged with the correlations decaying exponentially, while the long-ranged orientational correlations follow an algebraic decay. The isotropic liquid phase is characterized by short-ranged positional and orientational correlations.

Within KTHNY theory, the transition from the solid to the hexatic phase is accompanied by the unbinding of dislocation pairs into dislocations, while the hexatic to isotropic liquid transition occurs where the dislocations unbind into disclinations. However, the phase transition determined from the correlation functions may also occur at different parameter values than the onset of a certain type of defects, particularly if the phase transition is of first order contrary to KTHNY theory; see, e.g., Ref. [9] for anisotropic hard particles. Since here we study the effect of the anisotropy of the skyrmion-skyrmion interactions on the melting, we analyze the correlation functions and the number of topological defects separately, and compare their behavior with increasing temperature.

III. RESULTS

A. Skyrmion-skyrmion interaction

We calculate the interaction potential between pairs of skyrmions in the $(Pt_{0.95}Ir_{0.05})$/Fe/Pd(111) system as described in Sec. II A. We position the skyrmions along the nearest-neighbor $[1\bar{1}0]$ and the next-nearest-neighbor $[2\bar{1}\bar{1}]$ directions on the atomic lattice, so that the restriction that the centers of the skyrmions are fixed at lattice sites results in the densest distribution of points. The obtained interaction potentials are shown in Fig. 1. We fit the potential curves to the model function

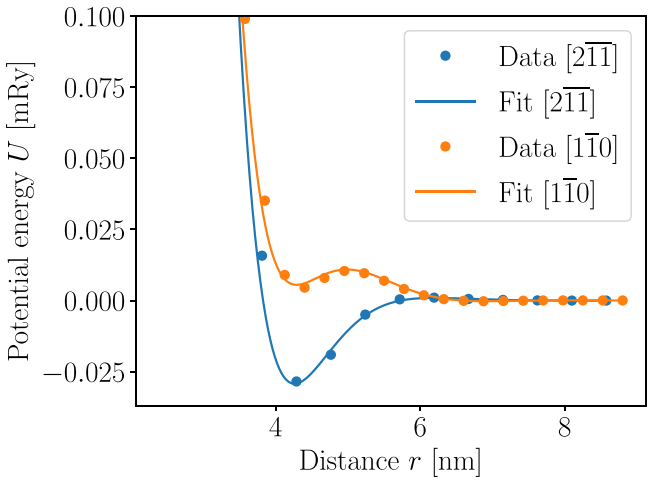

FIG. 1. Interaction potential between two skyrmions in the $(Pt_{0.95}Ir_{0.05})$/Fe/Pd(111) system at $B = 1$ T along the $[2\bar{1}\bar{1}]$ and $[1\bar{1}0]$ directions. Dots denote simulation data points, whereas lines indicate fits according to Eq. (8).

$$U(r_i) = e^{-\kappa_i r_i}(A_i \cos(k_i r_i + \phi_i) + B_i r_i + C_i), \tag{8}$$

where r_i is the absolute distance between the skyrmions along the direction $i \in \{[1\bar{1}0], [2\bar{1}\bar{1}]\}$. We show the obtained fitting values in Table I. Since the skyrmions are only about 10 lattice constants in diameter, the interaction between them is strongly affected by the geometry of the underlying atomic lattice. The isotropic exchange interactions between the atomic spins along the $[1\bar{1}0]$ and $[2\bar{1}\bar{1}]$ directions are ferromagnetic and antiferromagnetic, respectively [35]. Therefore, we get different potential curves along the $[2\bar{1}\bar{1}]$ and $[1\bar{1}0]$ directions, similarly to the $(Pt_{0.90}Ir_{0.10})$/Fe/Pd(111) system with slightly different composition in Ref. [35]. The interaction potential asymptotically follows an exponential decay modulated by an oscillating function due to the competition between the ferromagnetic and antiferromagnetic isotropic exchange interactions in the system [34]. This results in alternating repulsive and attractive parts of the potential, with the first potential minimum being much more shallow along the $[1\bar{1}0]$ than the $[2\bar{1}\bar{1}]$ direction. At the particle densities where the melting transition can be observed, the skyrmions are expected to explore only a small part of the interaction potential [7],

TABLE I. Interaction potential fit parameters for $(Pt_{0.95}Ir_{0.05})$/Fe/Pd(111) according to Eq. (8). Graphical representation can be seen in Fig. 1.

Parameter	Value $i = [2\bar{1}\bar{1}]$	Value $i = [1\bar{1}0]$
κ_i	1.8491 nm^{-1}	1.5449 nm^{-1}
A_i	−128.3853 mRy	19.9772 mRy
k_i	1.5525 nm^{-1}	2.1950 nm^{-1}
ϕ_i	−1.1404	0.1404
B_i	0.6074 mRy nm^{-1}	−5.3562 mRy nm^{-1}
C_i	8.9024 mRy	46.4040 mRy

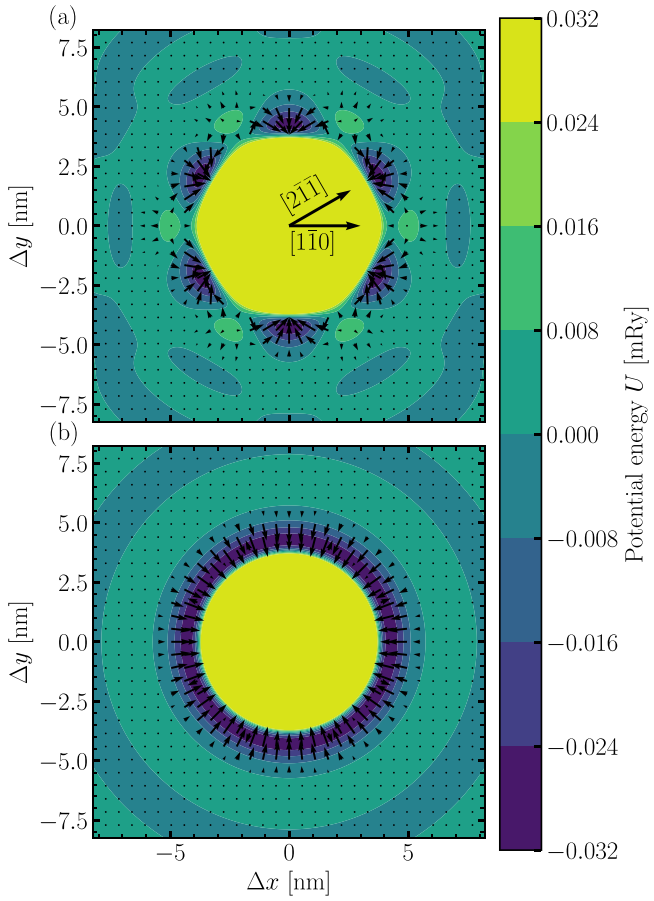

FIG. 2. Interaction potentials between two skyrmions in the $(Pt_{0.95}Ir_{0.05})$/Fe/Pd(111) system at $B = 1$ T. (a) Anisotropic interaction potential obtained by interpolating between the fits along the high-symmetry directions in Fig. 1 using the function in Eq. (9). (b) Isotropic potential obtained from the fit along the $[2\bar{1}\bar{1}]$ direction in Fig. 1. Arrows indicate the forces in the potential landscape.

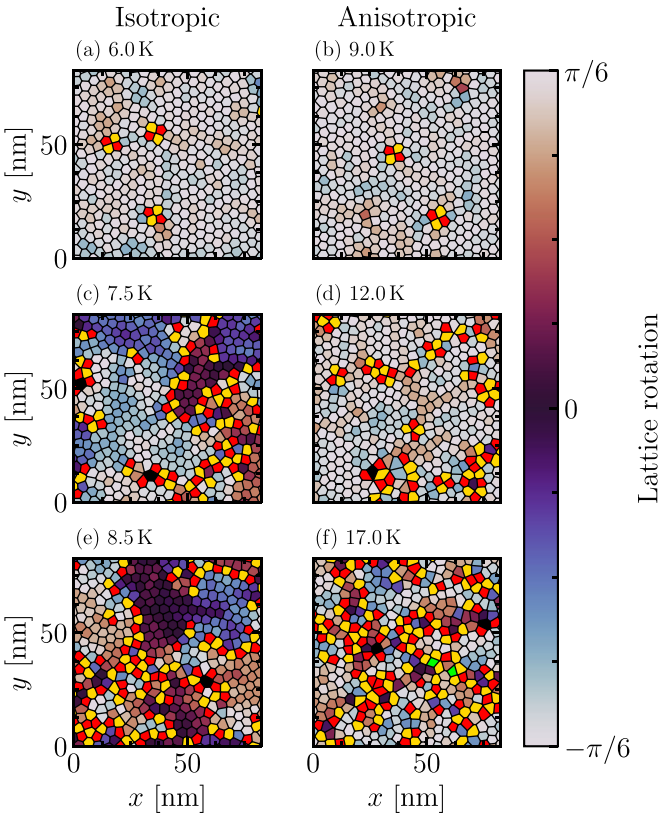

FIG. 3. Examples of simulations of skyrmion ensembles. (a), (c), (e) System with isotropic interactions. (b), (d), (f) System with anisotropic interactions. The simulation temperatures are indicated in each panel. Skyrmions with five and seven neighbors forming lattice defects are colored orange and yellow, respectively. Skyrmions with six neighbors, where the orientational order parameter $|\Psi_6(\boldsymbol{r}_i)|$ is close to unity, are colored according to the local lattice orientation $\arg \Psi_6(\boldsymbol{r}_i)$ as shown in the color bar.

meaning that these first potential minima are likely to play a decisive role in determining the nature of the transition. To generate a potential in two-dimensional space required for the quasiparticle dynamical simulations, we interpolate between the curves along the $[1\bar{1}0]$ and $[2\bar{1}\bar{1}]$ directions in the in-plane polar angle φ as

$$U(\boldsymbol{r}) = \cos^2(3\varphi)U_{[1\bar{1}0]}(r) + \sin^2(3\varphi)U_{[2\bar{1}\bar{1}]}(r), \qquad (9)$$

$$\text{with} \quad \boldsymbol{r} = \begin{pmatrix} r\cos\varphi \\ r\sin\varphi \end{pmatrix}. \qquad (10)$$

The interpolated potential is shown in Fig. 2(a). We see that the interaction potential has a sixfold symmetry reflecting the underlying triangular lattice, and that the skyrmions prefer to form bonds along the $[2\bar{1}\bar{1}]$ or symmetrically equivalent directions. At small distances r, we replace the interpolated potential (9) with a high constant value. The skyrmions are unable to explore this part of the interaction potential during the quasiparticle simulations, since it is separated by an extremely high energy barrier from the region at higher separation of the skyrmions. For comparison with this anisotropic interaction potential, we also construct an isotropic potential by rotating the potential curve obtained along the $[2\bar{1}\bar{1}]$ direction around the out-of-plane direction, as illustrated in Fig. 2(b). Since the skyrmions preferably form bonds along the same $[2\bar{1}\bar{1}]$ direction in the anisotropic potential, the preferred distance between the skyrmions remains the same between the two potentials along with the radial restoring forces, enabling us to primarily investigate the role of the anisotropy of the potential on the melting process.

B. Simulation of the melting transition

We performed quasiparticle dynamics simulations following the procedure described in Sec. II B using the two types of interaction potentials determined above. Figure 3 shows real-space representations of the simulations at selected temperature values, with the lattice defects highlighted and the phase of the orientational order parameter $\arg \Psi_6$ color coded. The orientation is calculated relative to the horizontal $[1\bar{1}0]$ atomic lattice direction. In panels (a) and (b), we see sections of configurations at relatively low temperatures clearly in the solid phase, with only nontopological dislocation pairs being visible and $\arg \Psi_6$ hardly varying over the simulation area. As we increase the temperature in the systems, we

observe the emergence of isolated dislocations in panels (c) and (d), indicative of a hexatic phase according to KTHNY theory. While the phase of the orientational order parameter slowly varies over the system for isotropic interactions, for the anisotropic interactions it remains close to $\arg \Psi_6 = \pi/6$; i.e., the bonds are still formed primarily along the $[2\bar{1}1]$ direction. Raising the temperature even further in panels (e) and (f), isolated disclinations appear in both systems, indicating a transition into the liquid phase within KTHNY theory. The phase $\arg \Psi_6$ varies rapidly for isotropic interactions in panel (e), indicating the loss of orientational order.

Note that the temperatures at which defect unbinding occurs also differ significantly between the two potentials. For the anisotropic interactions in panel (f), it can still be observed that the value of $\arg \Psi_6 = \psi/6$ is preferred, and the system does not become completely isotropic even at such elevated temperatures. Note that this is different from the observations for anisotropic hard particles in Refs. [8–10], where the particles were allowed to rotate leading to isotropy in the liquid phase. In our simulations, the favorable directions for bond formation cannot rotate, because they are locked to the crystallographic axes of the underlying atomic lattice, which remains stable in the investigated temperature range. With that, our work is more closely linked to earlier works discussing phase transitions of particles on periodic substrates [3], although the spatially modulated potential created by the substrate is not considered in our simulations.

While at $T = 9$ K, the system with anisotropic interactions is still in the solid phase, the system with isotropic interactions has already melted into an isotropic liquid. This may in part be explained by a slightly larger core size for the anisotropic interaction: note that the hard core of the skyrmions visible in yellow color in Fig. 2 is hexagonal for anisotropic interactions, while it is circular for isotropic interactions. Since the circle is constructed in such a way to touch the sides of the hexagon from the inside, the cores in the case of anisotropic interactions cover a larger area, resulting in a denser packing for the same number of skyrmions. However, the preference for the formation of the bonds along the $[2\bar{1}1]$ directions probably plays a more important role in stabilizing the ordered phases. Since each skyrmion admits six neighbors at the six well-defined minima of the anisotropic interaction potential, the formation of lattice defects with a different number of neighbors costs more energy than for the isotropic interactions where the skyrmions can be more easily displaced along the azimuthal direction.

For a more quantitative description of the defects during the melting process, we counted the number of isolated topological lattice defects and averaged over simulation time for different temperatures, which can be seen in Fig. 4. Note that we strictly only regard dislocations as pairs of skyrmions with five and seven neighbors, and disclinations as skyrmions with a number of neighbors different from six, both of which are surrounded by skyrmions with exactly six neighbors. This excludes other types of defects from the statistics, including dislocation pairs in the solid phase but also larger clusters of defects emerging at higher temperatures. We find for the isotropic interaction that the first dislocations appear at $T = 7$ K and the first disclinations at $T = 8$ K. The number of defects increases to a maximum in a very narrow temperature range for both types. Due to the strict classification of defects, we see that the number of defects starts decreasing above $T = 12$ K after a relatively constant region, which is not due to an increase in order in the system, but rather to the emergence of larger clusters that fall outside of our classification. The unbinding of defects according to KTHNY theory indicates a very narrow hexatic phase with dislocations but no disclinations between $T = 7$ K and $T = 8$ K. For anisotropic interactions, the first dislocations appear only at $T = 10$ K, while disclinations form above $T = 12$ K, restricting the hexatic phase into this temperature regime according to the above classification. The number of defects saturates in a considerably wider temperature range and reaches a lower maximum value than for the isotropic interactions, supporting the argument above that it is more difficult to form topological defects for anisotropic interactions with preferred bond orientations with respect to the atomic lattice. We start the analysis of the correlation functions with the structure factor from Eq. (7), shown in Fig. 5. At low temperature, we identify sharp peaks at the reciprocal-lattice vectors of the solid phase for both isotropic [Fig. 5(a)] and anisotropic [Fig. 5(b)] interactions. With increasing temperature in panels (c) and (d), the peaks widen along the azimuthal direction, and also along the radial direction primarily for peaks further away from the center. This hints at the loss of quasi-long-ranged positional order, while orientational order is preserved to an extent, which is consistent with a hexatic phase [16]. The most pronounced difference between the different types of interactions is shown in Figs. 5(e) and 5(f): for isotropic interactions, rings with uniform intensity can be observed around the center, which signals a transition into the isotropic liquid phase. However, the sixfold symmetry of the structure factor is preserved for

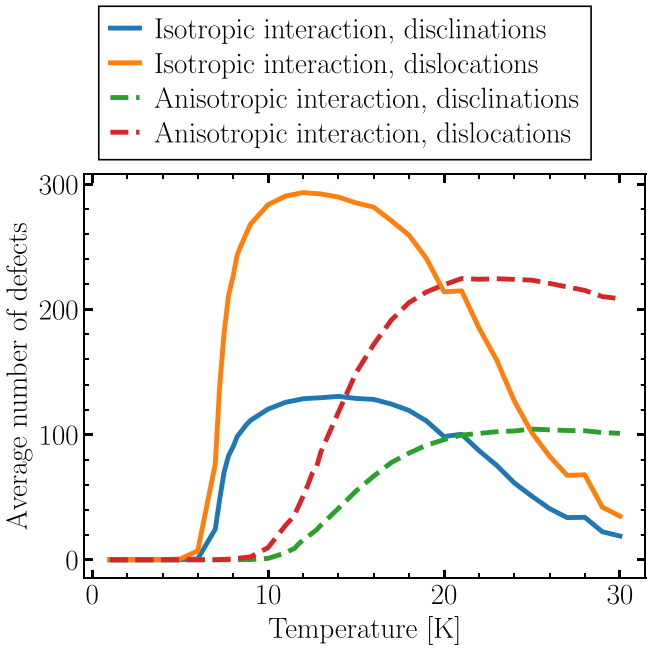

FIG. 4. Average number of topologically nontrivial defects as a function of temperature. Solid lines show results for a system with isotropic interactions and dashed lines for a system with anisotropic interactions.

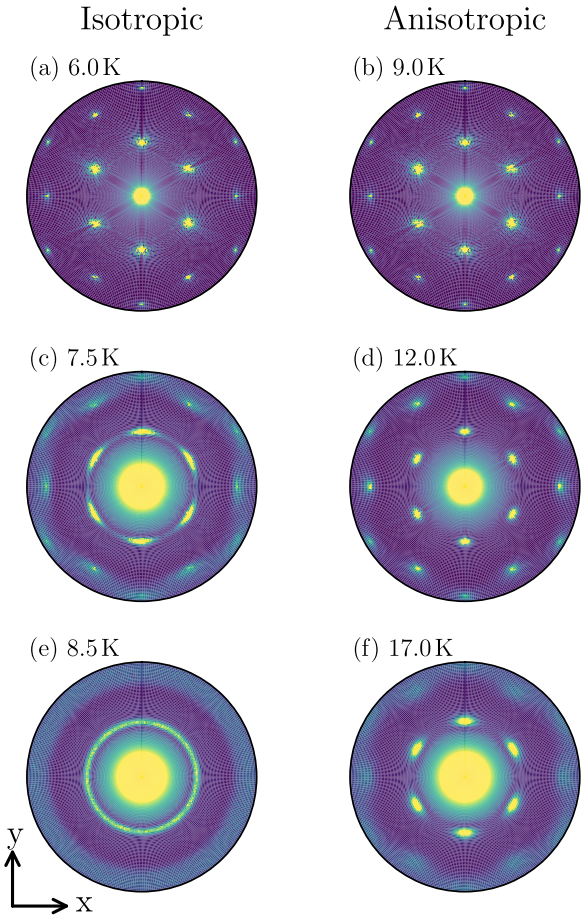

FIG. 5. Structure factor $S(\boldsymbol{q})$ calculated via Eq. (7). (a), (c), (e) System with isotropic interactions. (b), (d), (f) System with anisotropic interactions. Simulation temperatures are indicated in each panel.

anisotropic interactions up to $T = 17$ K, where there is already a very high number of dislocations and disclinations in the system (cf. Fig. 4). This high-temperature liquid phase still shows signatures of the preferred bond orientations induced by the atomic lattice.

In Fig. 6, the temperature dependence of the spatial orientational correlation function from Eq. (4), the temporal orientational correlation function from Eq. (5), and the maxima of the positional correlation function from Eq. (6) are shown for the two types of interaction potentials. At the lowest temperature for both the isotropic ($T = 6$ K) and the anisotropic ($T = 10$ K) interactions, the spatial and temporal orientational correlation functions converge to a finite value, while the positional correlation function decays algebraically, identifiable as a linear decrease in the log-log plots. These signatures are indicative of the solid phase. At $T = 7.5$ K for the system with isotropic interactions, both $g_6(r)$ and $g_6(t)$ decay algebraically, while the positional correlation function decays exponentially, which is faster than the linear decay in the log-log plot. This indicates a quasi-long-ranged orientational and short-ranged positional order, consistent with a hexatic phase. Contrary to this scenario, for anisotropic interactions the orientational correlation function converges to a finite value both at $T = 12.5$ K and at $T = 17$ K, with this order parameter decreasing with increasing temperature. The positional order is also short ranged for the anisotropic interactions. In contrast, the orientational correlations also become short ranged at $T = 8$ K for the isotropic interactions, indicating a transition into the isotropic liquid phase in agreement with the conclusions drawn from the unbinding of defects.

We calculated the average bond order parameter $|\langle\Psi_6\rangle|$, as shown in Fig. 7. While in the system with isotropic interactions, this order parameter reaches zero at around $T = 8$ K as the system transforms into the isotropic liquid phase, in the system with anisotropic interactions the orientational order persists at all investigated temperatures up to 30 K. The exponential decay as seen in the inset suggests a persistence to even higher temperatures within the scope of validity for our model.

Overall, for the isotropic interactions the correlation functions indicate two phase transitions: first from a solid phase with quasi-long-ranged positional and long-ranged orientational order to a hexatic phase with short-ranged positional and quasi-long-ranged orientational order at $T \approx 7$ K, and then from the hexatic to the isotropic liquid phase where all correlations are short ranged at $T \approx 8$ K. The change in the decay of the correlation functions agrees with the onset of first the dislocations and then the disclinations in Fig. 3. These observations are consistent with KTHNY theory. For the anisotropic interactions, we find that the anisotropy induced by the atomic lattice enforces orientational order in the system at all investigated temperatures. The positional correlation function changes from an algebraic to an exponential decay at $T \approx 11$ K. This agrees with an inflection point in the orientational order parameter in Fig. 7, above which it decays exponentially. We find no other signature of a phase transition and identify the low-temperature phase as a solid and the high-temperature phase as a liquid with anisotropic skyrmion orientations induced by the interaction potential. Although the hexatic phase is also characterized by quasi-long-ranged orientational correlations, in the anisotropic case the orientational order is not caused by spontaneous symmetry breaking but by the atomic lattice. Therefore, the onset of dislocations and disclinations in Fig. 4 at different temperatures cannot be connected to two separate phase transitions, either.

C. Machine-learning classification of phases

We also used a machine-learning algorithm to identify possible phases during the melting transition. For this purpose, we rasterized the local bond-order parameter $\Psi_{6,i}$. We created a grid and averaged the complex argument $\arg(\Psi_{6,i})$ and the absolute value $|\Psi_{6,i}|$ for all skyrmions in each cell of the grid. Using periodic boundary conditions, each rasterization was then also shifted by a random amount in the x and y coordinates. This was done to minimize overfitting to a particular configuration of the skyrmion lattice. We used a rasterization grid of 40×40, where each cell had on average about 10.4 skyrmions in them. For finer grids, there was a chance of having no skyrmions in a cell, and coarser grids produced less separated clusters. The averaged local bond-order parameter was then used as an input for the k-means clustering algorithm

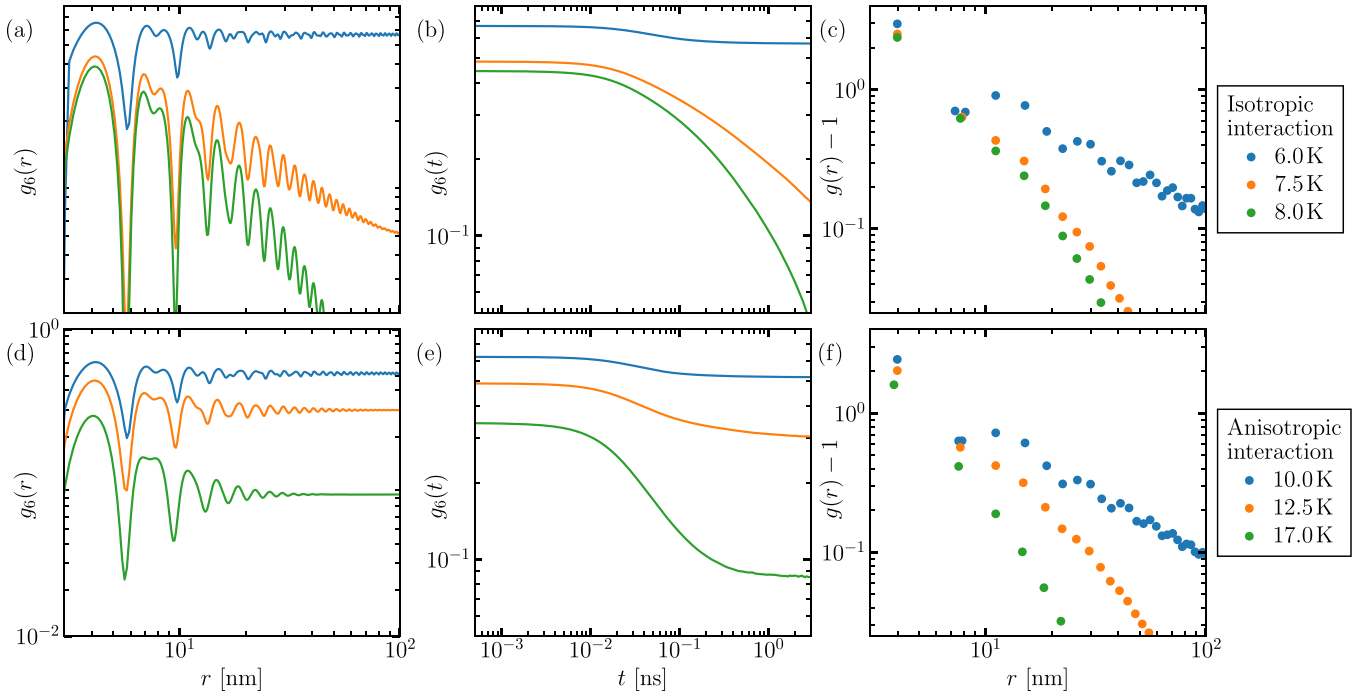

FIG. 6. Calculated correlation functions in the system. (a), (d) Spatial orientational correlation function $g_6(r)$, (b), (e) temporal orientational correlation function $g_6(t)$, and (c), (f) positional correlation function $g(r) - 1$, for both (a)–(c) the system with isotropic interactions and (d)–(f) the system with anisotropic interactions. The functions are plotted on a log-log scale to visually distinguish between algebraic and exponential decays. Only the local maxima of the oscillating function are shown in panels (c) and (f).

[42] with the implementation from the Python package scikit-learn [43] for identifying possible phases.

The phase diagrams deduced from the machine-learning algorithm are shown in Fig. 8. The algorithm identified a low-temperature and a high-temperature phase for both systems with isotropic and anisotropic interactions, respectively. Although the two datasets for different interactions were combined during the analysis, the algorithm managed to separate the two types of interactions, apart from a few outlying configurations. This is surprising in the low-temperature solid phases, where our previous analysis could not identify a clear difference. However, in the high-temperature limit, the isotropic liquid phase and the liquid phase with enforced orientational order were also separated by the algorithm. The two clusters in each figure are separated by an almost

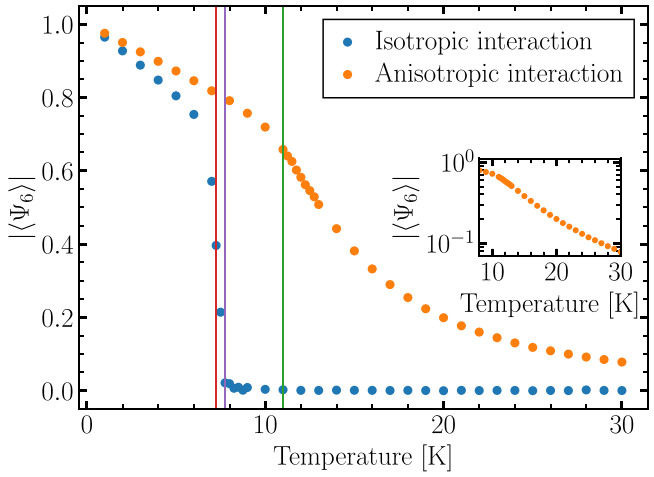

FIG. 7. Average bond order parameter $|\langle\Psi_6\rangle|$. Vertical lines show phase transitions determined from the decay of orientational and positional correlation functions. Red line denotes solid to hexatic transition and purple line hexatic to liquid transition for isotropic interaction ($T \approx 7$ K and $T \approx 8$ K, respectively). Green line denotes solid to anisotropic liquid transition for anisotropic interaction ($T \approx 11$ K). Inset shows the values for the anisotropic interactions on a logarithmic scale to visualize the exponential decay.

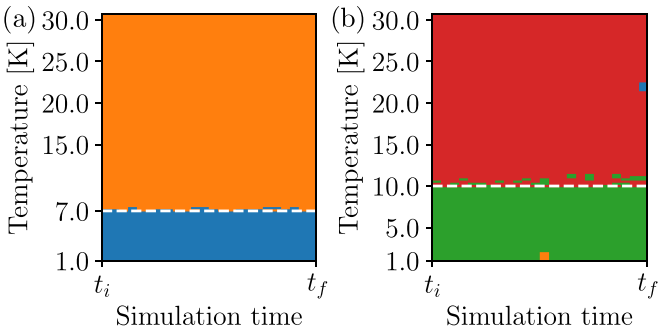

FIG. 8. Phase diagrams obtained from the machine-learning algorithm. Systems with isotropic and anisotropic interactions are shown in panels (a) and (b), respectively. Colors indicate the four different clusters. Along the horizontal axis different snapshots are shown from a simulation performed at a fixed temperature between initial time t_i and final time t_f. White dashed lines are guides to the eye identifying the critical temperatures of the predicted phase transitions.

horizontal line into a low-temperature and a high-temperature regime. Close to the transition line, configurations obtained from the same simulation may belong to different clusters; this may either be an indication for phase coexistence or designate data points located between two well-defined clusters. Note that the machine-learning algorithm only identified a single phase transition in both systems, correlating with the inflection point in the orientational order parameter in Fig. 7. It is possible that the algorithm could not separate the hexatic phase from the isotropic liquid phase for isotropic interactions because the former is found only in a narrow temperature range, which may contain an insufficient number of data points to be possible to be identified as a separate cluster. For the system with anisotropic interactions, the temperature of the single identified phase transition is close to the value determined from the analysis of the correlation functions above.

IV. CONCLUSIONS

We studied the influence of the anisotropy of the skyrmion-skyrmion interaction potential on the melting of the skyrmion lattice. We determined a spatially anisotropic interaction potential for skyrmions in the $(Pt_{0.95}Ir_{0.05})$/Fe/Pd(111) system from atomistic simulations, which prefers bond formation along the $[2\overline{11}]$ and symmetrically equivalent directions. For comparison, we also constructed an isotropic potential with the same depth of the potential minima. We performed dynamical simulations treating the skyrmions as quasiparticles to study the melting transition. By analyzing the topological defects in the system, we found an onset of dislocations at $T = 7$ K and at $T = 10$ K, and the appearance of disclinations at $T = 8$ K and at $T = 12$ K for systems with isotropic and anisotropic skyrmion-skyrmion interactions, respectively. We concluded that the preferred directions of bond formation in the anisotropic potential hinder the formation of defects, thereby increasing the stability of the ordered phase. From the analysis of the correlation functions, we found that quasi-long-range positional correlations persist in the system approximately up to the temperature where the dislocations appear for both types of interactions, identifying this low-temperature phase as a solid state. For the isotropic interactions, the orientational order remains quasi-long-ranged up to the onset of disclinations, making it possible to identify a second transition at around $T = 8$ K from a hexatic to an isotropic liquid phase. The observations for this system are in qualitative agreement with KTHNY theory. In contrast, we found that in the case of anisotropic interactions the orientational order parameter remains finite, only decreasing asymptotically with temperature. While quasi-long-ranged orientational order is characteristic of a hexatic phase instead of a liquid phase, here the order is enforced by the anisotropy of the interactions; therefore, we identified the high-temperature phase as a liquid with induced anisotropy for this system. We also characterized the obtained local orientational order parameters in the system using a machine-learning algorithm, which successfully distinguished between the two types of interactions and between solid and nonsolid phases, but could not identify the narrow temperature range where the hexatic phase was found previously for isotropic interactions.

Our simulations for skyrmions with short-range attraction found indications for a hexatic phase, similarly to previous experimental studies for skyrmions with purely repulsive interactions [26,27]. Further investigations of the system with isotropic interactions may be possible to elucidate the first-order or second-order nature of the phase transitions, which could clarify whether KTHNY theory or a competing interpretation is best applicable in this scenario. However, this will require increasing the number of particles in the simulations further, because the correlation lengths often reach very high values in similar simulations [9]. Further research could investigate tuning the skyrmion-skyrmion interaction potentials to widen the hexatic phase. This could include the computation of density-temperature phase diagrams.

Our simulations take the anisotropy in the interactions as a mechanism of breaking continuous rotational symmetry into account, and therefore differ from works with noncircular particle shapes that are allowed to rotate [8–10]. Instead, our work is more closely linked to particles within a periodic potential induced by the lattice.

Previous simulations for repulsive skyrmions with isotropic interactions in Ref. [29] found a direct transition from the solid to the isotropic liquid phase, which was attributed to the strong periodic potential exerted by the underlying atomic square lattice on the small-scale skyrmions. While this periodic potential was not considered in our quasiparticle simulations, the influence of the atomic lattice was taken into account in the anisotropy of the interactions. This also resulted in a direct solid-to-liquid transition, but sixfold orientational order also persisted in the liquid phase, in contrast to the isotropic liquid phase identified in Ref. [29].

Systems where skyrmions are stabilized by the competition between ferromagnetic and antiferromagnetic magnetic exchange interactions, such as the $(Pt_{0.95}Ir_{0.05})$/Fe/Pd(111) system studied here, offer further prospects for studying the role of the anisotropy in the phase formation of quasiparticles. For example, such systems allow for the stabilization of different types of particlelike spin configurations [34,44]. These include antiskyrmions, which besides having anisotropic interaction potentials, may also rotate on the atomic lattice [38], introducing a further degree of freedom that may influence the melting transition. The investigations could further be extended to ensembles containing both skyrmions and antiskyrmions, which have been demonstrated to prefer a nontriangular arrangement already in the solid phase [34].

ACKNOWLEDGMENTS

We would like to thank Markus Weißenhofer and Elena Y. Vedmedenko for fruitful discussions. We acknowledge funding by the Deutsche Forschungsgemeinschaft (DFG, German Research Foundation) via SFB 1432 and Projects No. 403502522 and No. 514141286, by the National Research, Development, and Innovation Office (NRDI) of Hungary under Project No. FK142601 and No. ADVANCED 149745, by the Ministry of Culture and Innovation and the National Research, Development and Innovation Office within

the Quantum Information National Laboratory of Hungary (Grant No. 2022-2.1.1-NL-2022-00004), and by the Hungarian Academy of Sciences via a János Bolyai Research Grant (Grant No. BO/00178/23/11). We are grateful for the computational support and resources provided by the Scientific Compute Cluster of University of Konstanz (SCCKN) for the simulations of the skyrmion lattices.

DATA AVAILABILITY

The data that support the findings of this article are not publicly available upon publication because it is not technically feasible and/or the cost of preparing, depositing, and hosting the data would be prohibitive within the terms of this research project. The data are available from the authors upon reasonable request.

[1] J. M. Kosterlitz and D. J. Thouless, Ordering, metastability and phase transitions in two-dimensional systems, J. Phys. C **6**, 1181 (1973).
[2] B. I. Halperin and D. R. Nelson, Theory of two-dimensional melting, Phys. Rev. Lett. **41**, 121 (1978).
[3] D. R. Nelson and B. I. Halperin, Dislocation-mediated melting in two dimensions, Phys. Rev. B **19**, 2457 (1979).
[4] A. P. Young, Melting and the vector Coulomb gas in two dimensions, Phys. Rev. B **19**, 1855 (1979).
[5] P. Bladon and D. Frenkel, Dislocation unbinding in dense two-dimensional crystals, Phys. Rev. Lett. **74**, 2519 (1995).
[6] E. P. Bernard and W. Krauth, Two-step melting in two dimensions: First-order liquid-hexatic transition, Phys. Rev. Lett. **107**, 155704 (2011).
[7] S. C. Kapfer and W. Krauth, Two-dimensional melting: From liquid-hexatic coexistence to continuous transitions, Phys. Rev. Lett. **114**, 035702 (2015).
[8] K. Wojciechowski and D. Frenkel, Tetratic phase in the planar hard square system? Comput. Methods Sci. Technol. **10**, 235 (2004).
[9] J. A. Anderson, J. Antonaglia, J. A. Millan, M. Engel, and S. C. Glotzer, Shape and symmetry determine two-dimensional melting transitions of hard regular polygons, Phys. Rev. X **7**, 021001 (2017).
[10] L. Walsh and N. Menon, Ordering and dynamics of vibrated hard squares, J. Stat. Mech. (2016) 083302.
[11] C. J. Guo, D. B. Mast, R. Mehrotra, Y. Z. Ruan, M. A. Stan, and A. J. Dahm, Evidence in support of dislocation-mediated melting of a two-dimensional electron lattice, Phys. Rev. Lett. **51**, 1461 (1983).
[12] N. N. Negulyaev, V. S. Stepanyuk, L. Niebergall, P. Bruno, M. Pivetta, M. Ternes, F. Patthey, and W.-D. Schneider, Melting of two-dimensional adatom superlattices stabilized by long-range electronic interactions, Phys. Rev. Lett. **102**, 246102 (2009).
[13] M. Cheng, J. T. Ho, S. W. Hui, and R. Pindak, Observation of two-dimensional hexatic behavior in free-standing liquid-crystal thin films, Phys. Rev. Lett. **61**, 550 (1988).
[14] C. A. Murray and D. H. Van Winkle, Experimental observation of two-stage melting in a classical two-dimensional screened Coulomb system, Phys. Rev. Lett. **58**, 1200 (1987).
[15] A. J. Armstrong, R. C. Mockler, and W. J. O'Sullivan, Isothermal-expansion melting of two-dimensional colloidal monolayers on the surface of water, J. Phys.: Condens. Matter **1**, 1707 (1989).
[16] A. H. Marcus and S. A. Rice, Observations of first-order liquid-to-hexatic and hexatic-to-solid phase transitions in a confined colloid suspension, Phys. Rev. Lett. **77**, 2577 (1996).
[17] K. Zahn, R. Lenke, and G. Maret, Two-stage melting of paramagnetic colloidal crystals in two dimensions, Phys. Rev. Lett. **82**, 2721 (1999).
[18] I. Guillamón, H. Suderow, A. Fernández-Pacheco, J. Sesé, R. Córdoba, J. M. De Teresa, M. R. Ibarra, and S. Vieira, Direct observation of melting in a two-dimensional superconducting vortex lattice, Nat. Phys. **5**, 651 (2009).
[19] I. Roy, S. Dutta, A. N. Roy Choudhury, S. Basistha, I. Maccari, S. Mandal, J. Jesudasan, V. Bagwe, C. Castellani, L. Benfatto, and P. Raychaudhuri, Melting of the vortex lattice through intermediate hexatic fluid in an *a*–MoGe thin film, Phys. Rev. Lett. **122**, 047001 (2019).
[20] R. Sharma, D. Rey, L. Longchambon, A. Perrin, H. Perrin, and R. Dubessy, Thermal melting of a vortex lattice in a quasi-two-dimensional Bose gas, Phys. Rev. Lett. **133**, 143401 (2024).
[21] A. N. Bogdanov and D. A. Yablonskii, Thermodynamically stable "vortices" in magnetically ordered crystals. The mixed state of magnets, Zh. Eksp. Teor. Fiz. **95**, 178 (1989) [Sov. Phys. JETP **68**, 101 (1989)].
[22] A. Bogdanov and A. Hubert, Thermodynamically stable magnetic vortex states in magnetic crystals, J. Magn. Magn. Mater. **138**, 255 (1994).
[23] S. Mülbauer, B. Binz, F. Jonietz, C. Pfleiderer, A. Rosch, A. Neubauer, R. Georgii, and P. Böni, Skyrmion lattice in a chiral magnet, Science **323**, 915 (2009).
[24] X. Z. Yu, Y. Onose, N. Kanazawa, J. H. Park, J. H. Han, Y. Matsui, N. Nagaosa, and Y. Tokura, Real-space observation of a two-dimensional skyrmion crystal, Nature (London) **465**, 901 (2010).
[25] R. Seshadri and R. M. Westervelt, Statistical mechanics of magnetic bubble arrays. II. Observations of two-dimensional melting, Phys. Rev. B **46**, 5150 (1992).
[26] P. Huang, T. Schönenberger, M. Cantoni, L. Heinen, A. Magrez, A. Rosch, F. Carbone, and H. M. Rønnow, Melting of a skyrmion lattice to a skyrmion liquid via a hexatic phase, Nat. Nanotechnol. **15**, 761 (2020).
[27] R. Gruber, J. Rothörl, S. M. Fröhlich, M. A. Brems, F. Kammerbauer, M.-A. Syskaki, E. M. Jefremovas, S. Krishnia, A. Sudbø, P. Virnau, and M. Kläui, Real-time observation of topological defect dynamics mediating two-dimensional skyrmion lattice melting, Nat. Nanotechnol. **20**, 1405 (2025).
[28] C. Reichhardt, C. J. O. Reichhardt, and M. V. Milošević, Statics and dynamics of skyrmions interacting with disorder and nanostructures, Rev. Mod. Phys. **94**, 035005 (2022).
[29] Y. Nishikawa, K. Hukushima, and W. Krauth, Solid-liquid transition of skyrmions in a two-dimensional chiral magnet, Phys. Rev. B **99**, 064435 (2019).

[30] D. Schick, M. Weißenhofer, L. Rózsa, J. Rothörl, P. Virnau, and U. Nowak, Two levels of topology in skyrmion lattice dynamics, Phys. Rev. Res. **6**, 013097 (2024).

[31] I. Dzyaloshinsky, A thermodynamic theory of "weak" ferromagnetism of antiferromagnetics, J. Phys. Chem. Solids **4**, 241 (1958).

[32] T. Moriya, Anisotropic superexchange interaction and weak ferromagnetism, Phys. Rev. **120**, 91 (1960).

[33] S.-Z. Lin, C. Reichhardt, C. D. Batista, and A. Saxena, Particle model for skyrmions in metallic chiral magnets: Dynamics, pinning, and creep, Phys. Rev. B **87**, 214419 (2013).

[34] A. O. Leonov and M. Mostovoy, Multiply periodic states and isolated skyrmions in an anisotropic frustrated magnet, Nat. Commun. **6**, 8275 (2015).

[35] L. Rózsa, A. Deák, E. Simon, R. Yanes, L. Udvardi, L. Szunyogh, and U. Nowak, Skyrmions with attractive interactions in an ultrathin magnetic film, Phys. Rev. Lett. **117**, 157205 (2016).

[36] J. Zázvorka, F. Jakobs, D. Heinze, N. Keil, S. Kromin, S. Jaiswal, K. Litzius, G. Jakob, P. Virnau, D. Pinna, K. Everschor-Sitte, L. Rózsa, A. Donges, U. Nowak, and M. Kläui, Thermal skyrmion diffusion used in a reshuffler device, Nat. Nanotechnol. **14**, 658 (2019).

[37] A. A. Thiele, Steady-state motion of magnetic domains, Phys. Rev. Lett. **30**, 230 (1973).

[38] M. Weißenhofer and U. Nowak, Diffusion of skyrmions: The role of topology and anisotropy, New J. Phys. **22**, 103059 (2020).

[39] D. Schick, M. Weißenhofer, L. Rózsa, and U. Nowak, Skyrmions as quasiparticles: Free energy and entropy, Phys. Rev. B **103**, 214417 (2021).

[40] P. Keim, G. Maret, and H. H. von Grünberg, Frank's constant in the hexatic phase, Phys. Rev. E **75**, 031402 (2007).

[41] S. Z. Lin, B. Zheng, and S. Trimper, Computer simulations of two-dimensional melting with dipole-dipole interactions, Phys. Rev. E **73**, 066106 (2006).

[42] J. B. McQueen, Some methods of classification and analysis of multivariate observations, in *Proceedings of the 5th Berkeley Symposium on Mathematical Statistics and Probability* (University of California Press, Berkeley, CA, 1967), pp. 281–297.

[43] F. Pedregosa, G. Varoquaux, A. Gramfort, V. Michel, B. Thirion, O. Grisel, M. Blondel, P. Prettenhofer, R. Weiss, V. Dubourg, J. Vanderplas, A. Passos, D. Cournapeau, M. Brucher, M. Perrot, and E. Duchesnay, Scikit-learn: Machine learning in Python, J. Mach. Learn. Res. **12**, 2825 (2011).

[44] L. Rózsa, K. Palotás, A. Deák, E. Simon, R. Yanes, L. Udvardi, L. Szunyogh, and U. Nowak, Formation and stability of metastable skyrmionic spin structures with various topologies in an ultrathin film, Phys. Rev. B **95**, 094423 (2017).